

Improved Treatment of Surface Evapotranspiration in a Mesoscale Numerical Model Part I: Via the Installation of the Penman-Monteith Method

Chia-Rong Chen¹ and Peter J. Lamb²

(Manuscript received 26 August 1997, in final form 8 December 1997)

ABSTRACT

The Pennsylvania State University/National Center for Atmospheric Research Mesoscale Model version 4 (PSU/NCAR MM4) system shows that the simplified bucket method pioneered by Manabe (1969) to parameterize surface evapotranspiration (ET) has an apparent tendency to overestimate surface ET during nighttime and daytime due to (1) the inappropriate assignment of a parameter called moisture availability (M) in the method, and (2) the use of the saturation mixing ratio at the skin temperature as the surface mixing ratio when the long-term observational data from the Atmospheric Radiation Measurement (ARM) program are used for verification. It is also noted that the degree of overestimating latent heat fluxes decreases with the forecasting time. This is the so-called 'spinup problem' that is common in many numerical models owing to the inadequate assignment of the initial skin temperature and the associated saturation surface mixing ratio.

A Penman-Monteith (PM) method of estimating potential ET is implemented into the modeling system and is shown to lead to a more reasonable estimation (less overestimation) of ET. The degree of overestimating or underestimating latent heat flux by the PM method is mainly controlled by the setting of stomatal resistance given a fixed M. Less surface evaporative cooling, as implied by the PM method, leads to a warmer skin temperature and, consequently, a stronger estimation of daytime sensible heat flux by the model. Compared with the bucket method, the PM method leads to a lower moisture supply from the model's ground surface; thus, there is less probability of low-level cloud formation. A more reasonable estimation of net radiation at the ground surface is then proven to be associated with the use of the PM method. This method restricts the moisture supply from the ground surface and enables the model to make a prediction of the amount and tendency of the mixing ratio at the lowest model level (about 40 meters

¹Meteorological Satellite Center, Central Weather Bureau, Taipei, Taiwan, ROC

²School of Meteorology, University of Oklahoma, Norman, Oklahoma, USA

above ground level), which is in more agreement with the corresponding observations.

(Key words: Evapotranspiration, Penman-Monteith method, Skin temperature, Moisture availability, ARM program)

1. INTRODUCTION

Surface evapotranspiration (ET), along with other surface heat budget terms, is one of the lower boundary conditions in numerical models, such as the Numerical Weather Prediction (NWP) models, mesoscale numerical models, General Circulation Models/ Global Climate Models (GCMs) and the single column models. It affects the formation process of low-level clouds or even deep convection (Segal *et al.* 1995). Since the studies of Walker and Rowntree (1977), Shukla and Mintz (1982), Yeh *et al.* (1984) and others, it has become more and more apparent that NWP models are sensitive to the parameterization of the surface exchange processes at the atmosphere-land surface interface. The development of the daytime planetary boundary layer is strongly dependent upon the parameterized surface sensible and latent heat fluxes. Convective precipitation over land is also sensitive to soil-moisture surface-evaporation parameterization. In daily short- and medium-range forecast applications, an inappropriate representation of the ET leads to errors in cloud predictions and land surface precipitation forecasts. Such forecasts can be greatly enhanced from a more realistic thermodynamic structure due to an improved estimation of the ET (Beljaars *et al.* 1996). Many NWP models-such as the one used in this study, the PSU/NCAR MM4,-utilize a simple bucket-type method pioneered by Manabe (1969) to parameterize the surface latent heat flux process. With this method, there is a bucket at each grid point, and the ET is reduced from a potential value by the ratio (or, the so-called 'moisture availability') of soil water in the bucket and a specified field capacity value. The potential ET is evaluated under the assumption that the soil is saturated at the model-calculated "skin" (ground surface) temperature. The bucket method tends to overestimate surface ET (Section 3). One scheme, however, based on the concepts proposed by Penman (1948) and Monteith (1965), can more reasonably parameterize the potential ET over land and is, therefore, implemented into the modeling system used in this research.

The principal interest of this research is to improve a numerical model's estimation of surface ET by using the long-term observational data set from the Southern Great Plains (SGP) Atmospheric Radiation Measurement (ARM) program site (Stokes and Schwartz, 1994) for verification. Given the correct radiative forcing at the surface, the land surface schemes are also largely responsible for the quality of model-produced near surface weather parameters, such as near surface temperature and dewpoint as well as low-level cloudiness. Furthermore, the surface conditions need to be such that they provide adequate feedback mechanisms for the other physical processes in the atmosphere: low-level cloudiness influences the surface radiative balance, and sensible heat and latent heat fluxes affect the boundary layer exchange processes. Similarly the intensity of moist convection is related to these near surface physical processes. A correct partitioning between sensible and latent heat fluxes is helpful in determining soil wetness which acts as one of the forcing mechanisms of low-frequency atmo-

spheric variability (Milly and Dunne, 1994).

In the following sections, the proposed Penman-Monteith (PM) method of estimating the potential ET over land area is outlined. The manner by which it affects the estimation of surface ET in the mesoscale numerical model is demonstrated. In Section 2, the description and derivation of the PM method is introduced. The observational data set used in this research and the basic statistical (long-term) performance in estimating surface ET by the model is presented in Section 3. The results from the use of the PM method are discussed in Section 4. Finally, the summary and conclusions from this research are stated in Section 5. A variational algorithm of assimilating satellite retrievals to improve a model's estimation of surface fluxes will be shown at a later date in Part II of this research project.

2. THE PENMAN-MONTEITH (PM) METHOD

Penman (1948) first put forth a formula to estimate potential ET, but that, the original formulation can now be further modified to include the effect of stomatal resistance for vegetation based on Monteith (1965). Following Mahrt and Ek (1984), and with potential ET defined as the ET that can be determined if the soil is completely wet under the same environmental conditions (i.e., net radiative flux at the ground surface and ground heat flux are not altered), a formula is derived here to calculate (parameterize) the potential ET based on the concepts proposed by both Penman and Monteith. It is presented in the following.

When the soil is saturated, a skin temperature T'_g can be defined such that the surface energy balance equation can be written as:

$$R_{\text{net}} - H_m - H_s(T'_g) - L_v E_p(T'_g) = 0 \quad (2.1a)$$

and

$$R_{\text{net}} = (1 - \alpha)S \downarrow + L_w \downarrow - \epsilon_g \sigma T_g'^4, \quad (2.1b)$$

where R_{net} is the net radiation flux at the ground surface; H_m is the ground heat flux (heat flow into the substrate); H_s is the sensible heat flux; L_v is the latent heat of vaporization; E_p is the potential evapotranspiration; α is the albedo; S is the solar constant, so $(1 - \alpha)S \downarrow$ is the net shortwave radiative flux; $L_w \downarrow$ is the downward longwave radiative flux; ϵ_g is the emissivity of the ground surface; σ is the Stefan-Boltzmann constant; and $\epsilon_g \sigma T_g'^4$ is then the outgoing longwave radiative flux from the ground surface.

Surface temperature in Equation (2.1) is written as T'_g to denote that it is a hypothetical temperature from the saturated state. In contrast, the actual surface energy balance is defined as follows:

$$R_{\text{net}} - H_m - H_s(T_g) - M L_v E_p(T_g) = 0, \quad (2.2)$$

where M is the moisture availability factor ranging from 0.0 to 1.0. The last term of Equation (2.2) is obtained from Equation (2.1a). The difference between the two skin temperatures, $T_g - T'_g$, can be greater than 10°K when the soil is dry. In the original bucket method, this difference is ignored by using T_g to calculate E_p , which then brings about an inappropriate estima-

tion of latent heat flux. In Equation (2.1a), the single unknown variable is therefore the skin temperature T'_g . Mahrt and Ek (1984) showed that Penman's potential ET formula can be derived by starting from Equation (2.1a) and ignoring the effect of skin temperature, T'_g , on the outgoing longwave radiative flux and the ground heat flux. Such elimination is precisely what was done by Penman (1948).

In the modeling system used in this research (the PSU/NCAR MM4), the sensible heat flux (H_s) and potential ET (E_p) are parameterized as:

$$H_s = c_{pm} \rho_a \kappa u_* \frac{\theta'_g - \theta_a}{\ln \frac{z_a}{z_o} - \psi_h} \quad (2.3)$$

and

$$E_p = \rho_a I^{-1} (q_{sat}(T'_g) - q_a) \quad (2.4)$$

where $I^{-1} = \frac{\kappa u_*}{\ln \left(\frac{\kappa u_* z_a}{K_a} + \frac{z_a}{z_l} \right) - \psi_h}$; c_{pm} is specific heat at constant pressure for moist air;

ρ_a is air density for the lowest model level; κ is the von Karman constant (0.4); u_* is friction velocity; θ'_g is potential temperature of saturated soil surface; θ_a is potential temperature of the lowest model level; z_a is the height of the lowest model level; z_o is roughness length; ψ_h is the nondimensional stability parameter based on the similarity theory; $q_{sat}(T'_g)$ is the saturation mixing ratio at T'_g ; q_a is the mixing ratio at the lowest model level; K_a is the molecular diffusivity; and Z_l is the depth of the molecular layer.

Using Taylor's expansion,

$$q_{sat}(T'_g) \approx q_{sat}(T_a) + \left(\frac{dq_{sat}}{dT} \right)_{T_a} (T'_g - T_a) \quad (2.5)$$

in which T_a is the temperature at the lowest model level. Also, given

$$\left(\frac{dq_{sat}}{dT} \right)_{T_a} = \frac{\epsilon L_v q_{sat}}{R T_a^2}, \quad [\text{Clausius-Clapeyron Equation}], \quad (2.6)$$

with $\epsilon = 0.622$, $R = 287.04$ Joule/(kg $^\circ$ K), and L_v = latent heat of vaporization, Teten's formula (Bolton, 1980) can be used to estimate q_{sat} . E_p can then be expressed as:

$$E_p = E_a + \rho_a I^{-1} \left(\frac{dq_{sat}}{dT} \right)_{T_a} (T'_g - T_a) \quad (2.7)$$

with $E_a = \rho_a I^{-1} [q_{sat}(T_a) - q_a]$.

Similarly, $\epsilon_g \sigma T_g'^4 \approx \epsilon_g \sigma T_a^4 + 4 \epsilon_g \sigma T_a^3 (T'_g - T_a)$.

R_{net} or Equation (2.1b) can be rewritten as:

$$R_{\text{net}} = (1 - \alpha)S \downarrow + L_w \downarrow - \epsilon_g \sigma T_a^4 - 4\epsilon_g \sigma T_a^3 (T'_g - T_a). \quad (2.8)$$

Using T'_g and T_a , H_s (Equation 2.3) can be calculated, such that:

$$L_v E_p = (1 - \alpha)S \downarrow + L_w \downarrow - \epsilon_g \sigma T_a^4 - 4\epsilon_g \sigma T_a^3 (T'_g - T_a) - H_m - c_{pm} \rho_a k u_* \frac{T'_g - T_a}{\ln \frac{z_a}{z_o} - \psi_h} \left(\frac{100}{P_{\text{sfc}}} \right)^{\frac{R}{C_p}} \quad (2.9)$$

where P_{sfc} (surface pressure) is in units of centibars (cb). Therefore,

$$T'_g - T_a = \frac{(1 - \alpha)S \downarrow + L_w \downarrow - \epsilon_g \sigma T_a^4 - L_v E_p - H_m}{4\epsilon_g \sigma T_a^3 + \frac{c_{pm} \rho_a k u_* (100/P_{\text{sfc}})^{\frac{R}{C_p}}}{\ln \frac{z_a}{z_o} - \psi_h}}. \quad (2.10)$$

Then,

$$L_v E_p = L_v E_a + \Delta \cdot \frac{(1 - \alpha)S \downarrow + L_w \downarrow - \epsilon_g \sigma T_a^4 - L_v E_p - H_m}{\gamma + 1}, \quad (2.11)$$

where

$$\Delta = \frac{L_v}{c_{pm}} \cdot \left(\frac{dq_{\text{sat}}}{dT} \right)_{T_a} \cdot \frac{\ln \frac{z_a}{z_o} - \psi_h}{\ln \left(\frac{k u_* z_a}{K_a} + \frac{z_a}{z_1} \right) - \psi_h} \cdot \left(\frac{100}{P_{\text{sfc}}} \right)^{\frac{R}{C_p}}$$

and

$$\gamma = \frac{4\epsilon_g \sigma T_a^3}{c_{pm} \rho_a k u_* (100/P_{\text{sfc}})^{\frac{R}{C_p}} / (\ln \frac{z_a}{z_o} - \psi_h)}$$

This means that

$$L_v E_p = \frac{[(1 - \alpha)S \downarrow + L_w \downarrow - \epsilon_g \sigma T_a^4 - H_m] \Delta + (1 + \gamma)L_v E_p}{\Delta + \gamma + 1} \quad (2.12)$$

Monteith (1965) and others suggested that, in the presence of plants, the stomatal resistance (r_s) must be included. In this research, the stomatal resistance r_s (as defined by the resistance under no water stress) is set at 90 sm^{-1} (following Monteith 1965, Pan 1990, Pan *et al.* 1996). As such:

$$L_v E_p = \frac{[(1 - \alpha)S \downarrow + L_w \downarrow - \epsilon_g \sigma T_a^4 - H_m] \Delta + (1 + \gamma)L_v E_p}{\Delta + (\gamma + 1)(1 + I^{-1}r_s)} \quad (2.13)$$

It should be noted that the above derivation of the PM method is aimed at obtaining potential ET. As for the predicted surface temperature (T_g), the MM4 uses a force-restore slab model based on the surface energy equation developed by Blackadar (1976):

$$C_g \frac{\partial T_g}{\partial t} = R_{\text{net}} - H_m - H_s - M L_v E_p,$$

where C_g is the thermal capacity of the slab per unit area ($\text{Jm}^{-2}\text{K}^{-1}$); the terms on the right hand side of this equation are the same as those on the left hand side of Equation (2.2).

The latent heat flux in the model is then $M^*L_v E_p$ with M being moisture availability in a particular model grid (the definition and variability of M is discussed in Section 3). In this manner, the water stress in the stomate is parameterized in the same form as the bare soil bucket method. In essence, the derivation of the PM method to estimate potential ET over the land area is based on the original concept of the bucket method except for the facts that the PM method:

- (1) excludes the use of the hypothetical saturation mixing ratio at ground surface to estimate the moisture gradient between the ground surface and the lowest model level;
- (2) includes the effect of stomatal resistance; and
- (3) uses surface energy balance as a bound to estimate the potential ET in each model grid.

Based on the above-stated procedure to obtain the formulation of the PM method, the potential ET estimated by the PM method is a function of R_{net} , H_m and H_s . Obvious, therefore, is that during the daytime, when H_m and H_s are positive, from the surface energy balance point of view (Equations 2.1 and 2.2), the upper bound of potential ET should be the net radiation at the ground surface. In contrast, the potential ET estimated by the bucket method tends to be unbounded as is demonstrated in Section 4.2.

3. THE MESOSCALE MODEL PERFORMANCE

The PSU/NCAR MM4, as described by Anthes and Warner (1978) and Anthes *et al.* (1987), is the modeling system used in this research. It contains various moist convective parameterization schemes and relatively detailed boundary layer processes (Blackadar 1976, Deardorff 1972). During the model simulations, an explicit moisture scheme (i.e., the variabil-

ity of water vapor, cloud water and rain water are predicted; Dudhia 1989), multiple model levels in the planetary boundary layer and the time dependent inflow/outflow lateral boundary conditions are used.

As explained in many classical papers (such as those by Blackadar 1976, Deardorff 1972) and Chen (1996), the surface ET is expressed as:

$$ET = - \rho L_v K_q \frac{\partial q}{\partial z}, \quad (3.1)$$

where ρ is the air density; L_v is the latent heat of vaporization; K_q is the turbulent diffusion coefficient of water vapor; and $\partial q / \partial z$ is the moisture gradient close to the ground surface. Surface ET from the land surface in the MM4 is parameterized by a bucket-type method, following the concept pioneered by Manabe (1969). The exact formulation for the calculation of latent heat flux used in the MM4 is based on the work by Carlson and Boland (1978) as shown in Equations 2.2 and 2.4. It is now demonstrated how greatly the model's estimation of surface ET is improved with the implementation of the PM method.

The estimated surface ET by the model is contrasted with the corresponding observations from the SGP ARM site. The measurement of surface ET and the associated observational error characteristics are discussed in Chen (1996). In addition, observational data, such as latent heat flux, sensible heat flux, net radiation flux at the ground surface, near surface air temperature, near surface moisture content and surface pressure, etc., taken from three observational stations in the SGP ARM site (i.e., E9 at 36.43°N, 98.28°W; E13 at 36.6°N, 97.48°W; and E15 at 37.13°N, 97.26°W, as shown in Figure 3.1) are averaged for January, April, July and October of 1995. These represent the mean state of the atmospheric surface layer and ground conditions in different seasons and are used for verification against model simulation results from the model grid that is closest to the 3 SGP ARM observation stations, which is located at 36.24°N and 97.64°W.

It may be considered remarkable that data from the 360 × 400 km domain of the SGP ARM site (centered at 36.73°N, 97.54°W) can readily reveal systematic errors in a complex numerical model. However, the accuracy of the forecast model over the dense US network, the representativeness of the SGP ARM surface data and the existence of a long time series to select weather regimes (such as sunny and non-rainy days in different seasons) make this kind of verification relatively straightforward. Often, errors at one or two grid points of the numerical model (closest to the SGP ARM site) are representative of continental-scale errors since they represent systematic errors in the model formulation. The variation in the MM4 is relatively smooth over the region of Kansas and Oklahoma and if an adjacent grid point in the model was chosen, similar conclusions would be certainly reached about the model errors (Betts *et al.*, 1993). It should be noted that several quantities used for verification against model results, such as ground surface (skin) temperature, temperature at about 40m above ground level (AGL) and mixing ratio at about 40m AGL (40m AGL is the model's lowest level in the atmosphere) are not directly observed at the SGP ARM site; on the contrary, they are derived from the two-level (one- and two-meter height) air temperatures and mixing ratios taken from the SGP ARM stations based on the atmospheric surface layer similarity theory (Paulson 1970, Nickerson and Smiley 1975, Benoit 1977). An iterative shooting scheme is

designed to determine these quantities. The detailed procedures can be found in Chen (1996).

A series of model runs using the Anthes/Kou (Anthes, 1977) cumulus parameterization scheme with a grid spacing of 100 km were executed for January, April, July and October of 1995 in order to understand the model's statistical (long-term) performance in estimating surface ET. The main purpose of this series of model runs was to examine the model's statistical characteristics in different seasons. The computational domain for the model is shown in Figure 3.2. The estimated surface ET from the model grid point closest to the 3 SGP observation stations (E9, E13 and E15) in the ARM site was stored during every time step (1.5 min) of the model's 72-hr integration. These model estimations of ET were processed to determine hourly average values. These hourly average ET values from the model were contrasted with the corresponding observations from the above-mentioned 3 SGP observation stations. Compari-



Fig. 3.1. Map of the Southern Great Plains ARM site. Observational data from E9, E13 and E15 (marked with stars) are used for verification in this research. The closest model grid to these 3 stations is marked with a cross.

sons of the root mean square (RMS) and mean percentage (%) error of surface ET were made based on 3 forecast periods: 1-24 hr, 25-48 hr and 49-72 hr, according to which:

$$\text{RMS error} = \sqrt{\frac{\sum_n (F_n - O_n)^2}{n}} \quad (3.2)$$

and

$$\text{mean \% error} = \frac{\sum_n F_n - \sum_n O_n}{\sum_n O_n} \times 100 \% , \quad (3.3)$$

where F, O and n stand for forecast values, observed values and total number of forecasts or observations evaluated, respectively. The results from the bucket method are illustrated in Figures. 3.3, 3.4 and 3.5 for different seasons. The RMS and percentage errors for estimating latent heat flux by the bucket method are listed in Tables 3.1, 3.2 and 3.3. The results from the PM method, also shown in Figures. 3.3, 3.4 and 3.5 and Tables 3.1, 3.2 and 3.3, are discussed in Section 4. It should be kept in mind that in the following discussion, nighttime is defined as 01 - 12Z or 19 - 06 local standard time (LST), while daytime is defined as 13 - 24Z (or 07 - 18LST) over the Kansas and Oklahoma area. Three facts are known from these Figures and Tables, as listed below.

- (1) There is a clear tendency for RMS errors to decrease with increased forecasting time in January, April, July and October 1995 except for the 49-72 hr forecast period in July. The

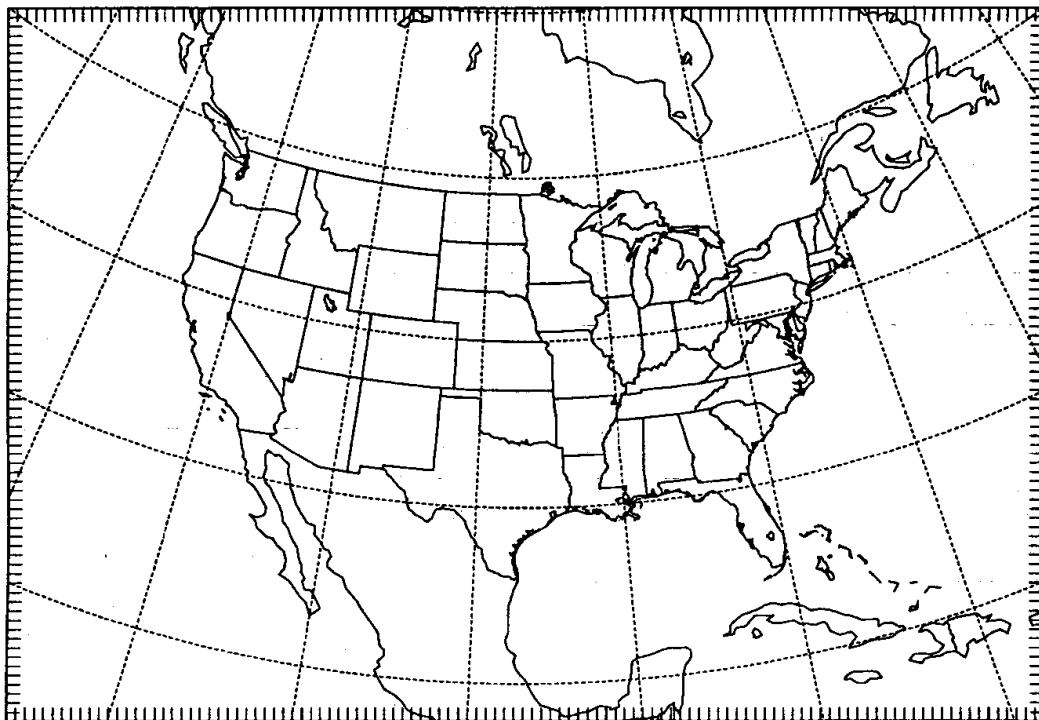


Fig. 3.2. The model's computational domain used in this study.

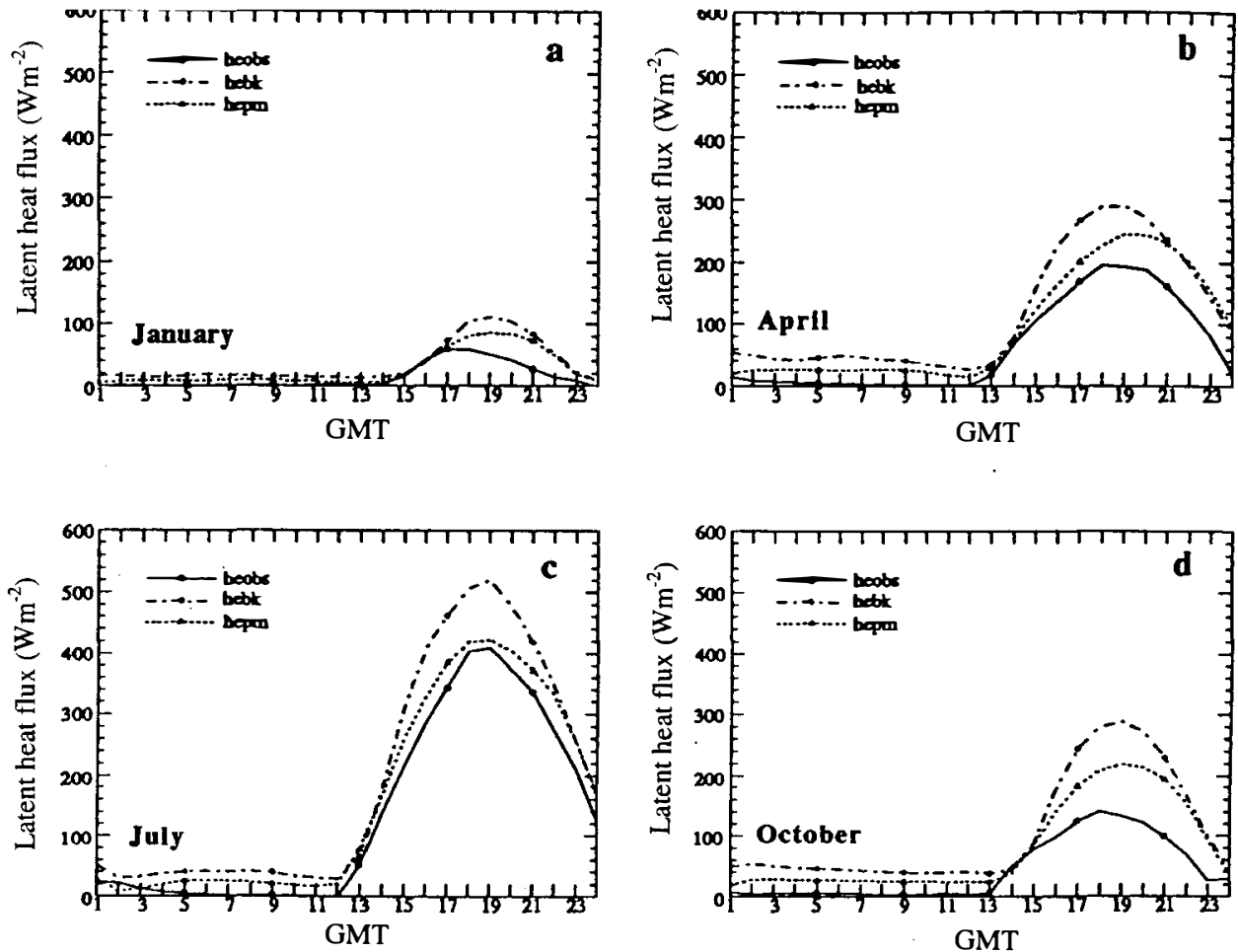


Fig. 3.3. Hourly average of the model estimation of latent heat flux (Wm^{-2}) in (a) January; (b) April; (c) July; and (d) October, 1995 during the model's 1-24 hour forecast period. The solid lines stand for the corresponding observation from the SGP ARM site, dashed lines for the model with the bucket method and the dotted lines for the model with the PM method as discussed in Section 4.

factor leading to an increase in the RMS error for the 49-72 hr forecast period in July is discussed in Section 4. The nighttime RMS errors are much smaller than daytime ones, but these differences decrease with increased forecasting time.

- (2) There is also a definite tendency for percentage errors to decrease with increased forecasting time. The mean percentage errors for nighttime are evidently greater than those for daytime.
- (3) Together with the RMS error analysis, it appears that the model has a higher variability in the estimation of nighttime surface ET than that for daytime. Thus, it can be said that the model has a greater chance of capturing the trend of surface ET in daytime.

From the above discussion, it is clear that the model using the bucket method is better able to adequately estimate latent heat flux as the forecasting time is extended. Both the percentage and RMS errors decrease with increased forecasting time, which is due to the spinup effect resulting from the inadequate assignment of the initial skin temperature and accompanying

Table 3.1. Percentage and RMS errors of model estimations of latent heat flux in (a) January; (b) April; (c) July; and (d) October 1995 during the model's 1-24 hr forecast period. Night is defined as from 01Z to 12Z, day from 13Z to 24Z and the total from 01Z to 24Z. The results from the PM method are discussed in Section 4.

	Bucket method			PM method		
	night	day	total	night	day	total
(a) January						
% error	3539.0	103.4	158.5	1797.0	66.8	94.6
RMS error	15.3	35.6	27.4	7.8	24.4	18.1
(b) April						
% error	804.1	56.0	83.7	408.2	36.5	50.2
RMS error	38.0	73.8	58.7	19.7	51.0	38.6
(c) July						
% error	446.0	30.1	40.6	204.4	13.5	18.3
RMS error	31.5	86.7	65.2	17.8	37.7	29.5
(d) October						
% error	859.2	102.3	142.9	465.6	63.0	84.6
RMS error	39.7	99.8	75.9	21.6	62.4	46.7

moisture gradient at the model's ground surface. There is no routine surface observation on the skin temperature. The model is initialized with a skin temperature and the associated moisture gradient at the ground surface which are both extrapolated from coarse conventional sounding and surface observational data. Hence, in the beginning of simulation, the model cannot well determine the skin temperature and the associated saturation surface mixing ratio used to calculate potential ET (see Equations 2.2 and 2.4) in the bucket method. It is evident, therefore, that the model makes a very poor estimation of ET initially. As the forecasting time is extended, however, the model gradually adjusts its simulation of skin temperature and the associated moisture gradient at the ground surface in accordance with surface energy balance constraints. In other words, an improved calculation of ET is shown to result from the adjustment of skin temperature and from a more reasonable (better) estimation of the associated moisture gradient between the ground surface and lowest model level, as the forecasting time is extended.

In the simple bucket method used in the MM4, the latent heat flux from the land surface is parameterized using the bulk-aerodynamical formula, as shown by Equations (2.2) and (2.4). In Equation (2.2), the factor M is defined as the ratio between the soil moisture content and

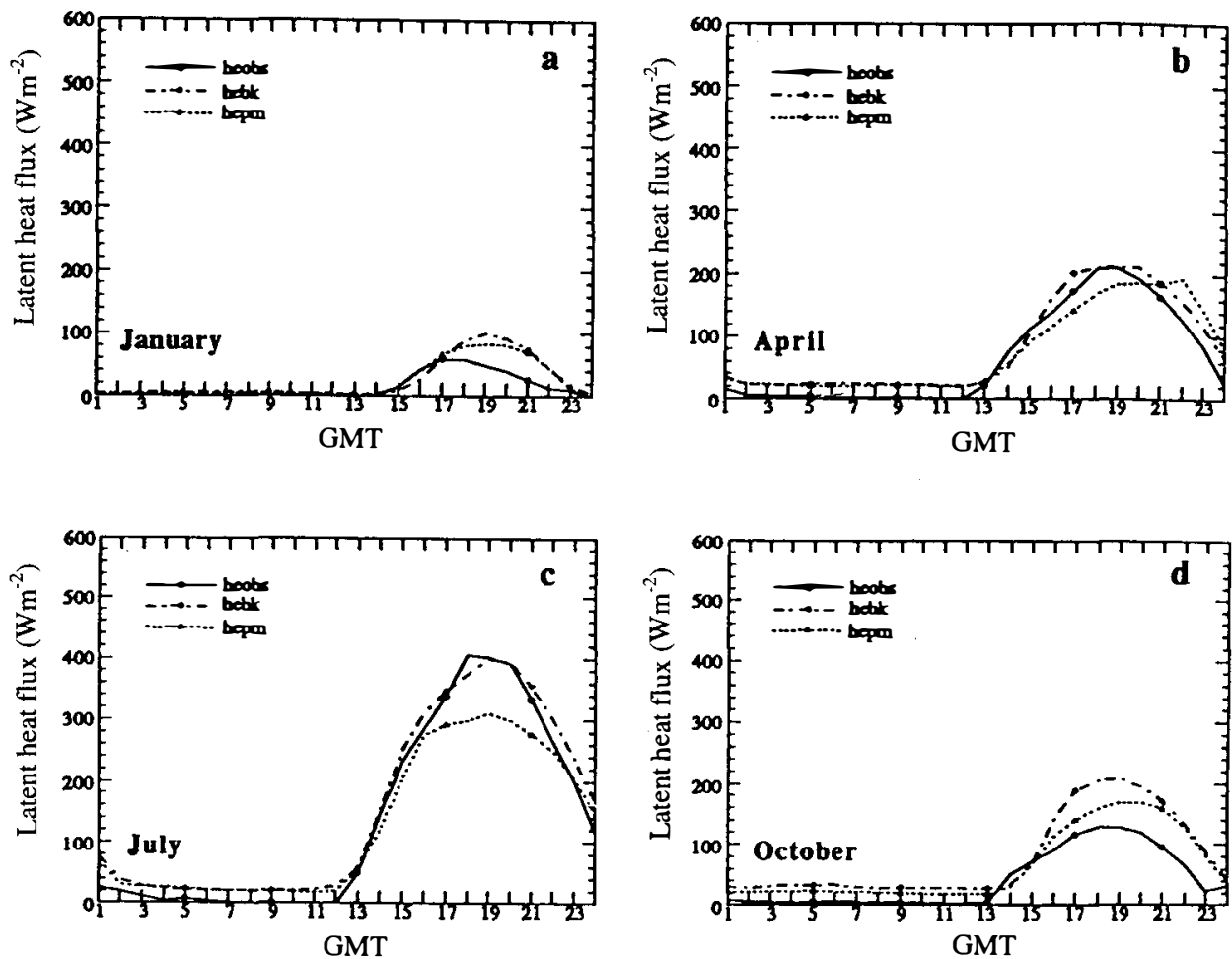


Fig. 3.4. Same as Figure 3.3 but for the model's 25-48 hr forecast period.

field capacity in a particular model grid and has a value between 0.0 and 1.0. The two key assumptions made in this method are:

- (1) the employment of a single parameter, M , to simulate the reduction of ET when the soil and vegetation are under stress, and
- (2) the use of the saturation mixing ratio at skin temperature as the surface mixing ratio.

Moisture availability (M) is regarded as the ratio of actual ET to its potential value. The concept of moisture availability was first suggested by Tanner and Pelton (1961) and later elaborated upon by Nappo (1975). This parameter basically expresses the efficiency of surface evaporation and is a fraction of the maximum possible evaporation for a saturated surface. M can be conceived as a measure of water saturation at ground surface. The use of the moisture availability concept is necessitated by the fact that the air layer in contact with the ground is not saturated except in those cases where the surface of the terrain is essentially saturated with water. The factor M is introduced to account for the reduction in the efficiency of evaporation due to the subsaturation of the ground surface. M probably approaches 1.0 over natural surfaces following a substantial rainfall, but for dry conditions or over artificial surfaces, such as concrete or developed urban areas, M may be quite low and basically independent of rainfall except for short periods following precipitation. For vegetation, M is related to the internal

Table 3.2. Same as Table 3.1 but for the model's 25-48 hr forecast period.

	Bucket method			PM method		
	night	day	total	night	day	total
(a) January						
% error	313.1	69.5	111.0	258.4	62.4	97.2
RMS error	8.0	29.2	21.4	6.6	23.2	17.1
(b) April						
% error	597.3	11.1	26.4	540.8	2.8	16.9
RMS error	20.5	23.1	21.9	18.6	36.7	29.1
(c) July						
% error	375.0	5.7	14.8	342.1	-13.7	-5.6
RMS error	24.8	25.5	25.2	22.2	54.9	41.9
(d) October						
% error	533.1	62.6	90.1	340.3	37.1	54.8
RMS error	25.6	58.9	45.4	16.4	38.9	29.8

resistance (bulk stomatal diffusion resistance) discussed by Monteith (1975). Over vegetated terrain, M may also decrease with prolonged dryness and fall rather rapidly to low values after the wilting point is reached. M is shown to be a complex function of soil type, canopy, vegetation, season and so on. (Taconet *et al.* 1986, Wetzels and Chang 1988, Gillies and Carlson 1995) In the bucket method, M is set to an empirical value as a function of land use and season, which on a daily basis tends to be far from reality. When the soil is wet, some stomatal resistance still remains in the plants which reduces ET from its potential value. When the soil is dry, ground surface temperature tends to be too high due to solar heating during the daytime, for example. Using it to determine the saturation surface mixing ratio, therefore, results in an overestimation of the potential value. In both situations, either wet or dry, the bucket method tends to overestimate ET, as illustrated in the above composite study of model runs.

It is also shown in Section 4 that the MM4 tends to have a warmer lower atmosphere during nighttime, which would lead to stronger downward longwave radiation (greenhouse effect) during nighttime such that the model's nighttime skin temperature would tend to be warmer than the corresponding observation (see Figure 4.3, as one example). This causes the saturation mixing ratio at skin temperature during nighttime to be high - even higher than the mixing ratio at the lowest model level. Water molecules underground then have extra kinetic energy to get into the air; thus, there is always ET coming from the model's ground surface during nighttime though the observations show near zero ET (see Figure 3.3, for instance).

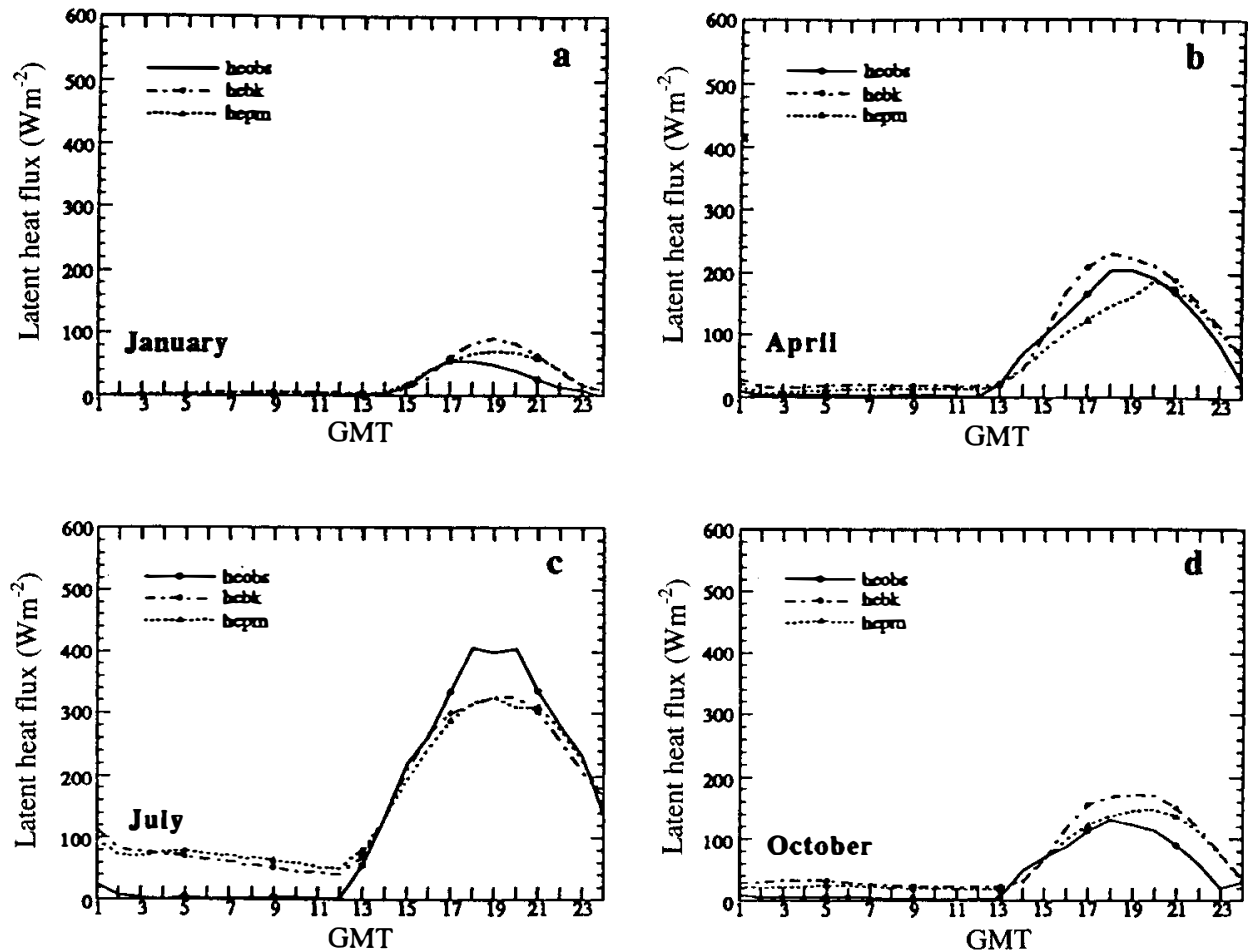


Fig. 3.5. Same as Figure 3.3 but for the model's 49-72 hr forecast period.

4. THE EFFECT OF PENMAN-MONTEITH METHOD

The Penman-Monteith (PM) method to calculate the potential ET over land area is implemented into the MM4 in hope of improving the model's estimation of latent heat flux. Observational data taken from three observation stations in the SGP ARM site are averaged for January, April, July and October 1995 to serve as the mean state of atmospheric surface layer and ground conditions. Seventy-two-hour model simulations are executed during the same months. The hourly averages of the model output at a grid point that is closest to the 3 observation stations are compared to the corresponding observational data set. It should be noted that surface fluxes, temperature and moisture during the daytime are discussed more frequently than those during the nighttime in the following discussion since errors related to these surface fluxes during the daytime can penetrate over deep layers and therefore affect the synoptic pressure fields (Beljaars *et al.*, 1996). Conversely, errors related to nighttime surface fluxes can only affect very shallow (near surface) layers. Hourly averages of the model's estimation of latent heat flux, sensible heat flux, net radiation at the ground surface (Equation 2.1b), the ground surface (skin) temperature and temperature and moisture content at about 40m AGL (the lowest model level in the atmosphere) at the SGP ARM site are determined and shown with their corresponding observations. The corresponding mean percentage errors and RMS errors for various fluxes, temperatures and moisture in 3 forecast periods are also selectively given.

Table 3.3. Same as Table 3.1 but for the model's 49-72 hr forecast period.

	Bucket method			PM method		
	night	day	total	night	day	total
(a) January						
% error	987.6	64.6	84.0	1053	50.7	71.1
RMS error	4.7	23.9	17.2	4.8	17.2	12.6
(b) April						
% error	358.5	15.2	26.0	178.3	-9.7	-3.7
RMS error	14.8	27.1	21.8	7.7	30.6	22.3
(c) July						
% error	1158	-10.3	11.7	1241	-10.5	13.1
RMS error	61.4	45.3	53.9	64.2	47.9	56.6
(d) October						
% error	474.7	44.4	70.4	345.2	26.8	46.1
RMS error	22.8	41.8	33.7	16.5	29.7	24.0

4.1 For 1-24 hr Forecast Period

The bucket method has a tendency to overestimate latent heat flux (LHF) by 103%, 56%, 30% and 102% during the daytime in January, April, July and October, respectively, during the first 24-hr forecast period (Figure 3.3 and Table 3.1). However, the PM method effectively reduces the potential ET (PE) (by 17%, from 53 Wm^{-2} with the bucket method to 44 Wm^{-2} with the PM method in January, for instance) by setting an upper bound to the PE. It causes the model to overestimate LHF by only 67%, 37%, 14% and 63% in January, April, July and October, respectively, during the daytime. The RMS errors for LHF are also decreased when the PM method is in use. For example, in July the RMS error for LHF is 65 Wm^{-2} with the bucket method but 29 Wm^{-2} with the PM method.

Since there is too much evaporative cooling associated with the bucket method, it follows that the surface temperature is too cold during the daytime. To illustrate, the mean skin temperature in the model using the bucket method is 20% colder than the corresponding observation in January. The model with the PM method, on the other hand, generates less LHF, thereby producing a higher daytime skin temperature and subsequently a higher daytime sensible heat flux (SHF). In January and April, the bucket method is associated with a mean daytime skin temperature of 5.1 and 16.3°C, respectively (Figure 4.3 and Table 4.3). Whereas, the PM method is associated with a mean daytime skin temperature of 5.6 and 18.7°C, respectively. Observations, in fact, show a mean skin temperature of 6.3 and 20.0°C in January and April,

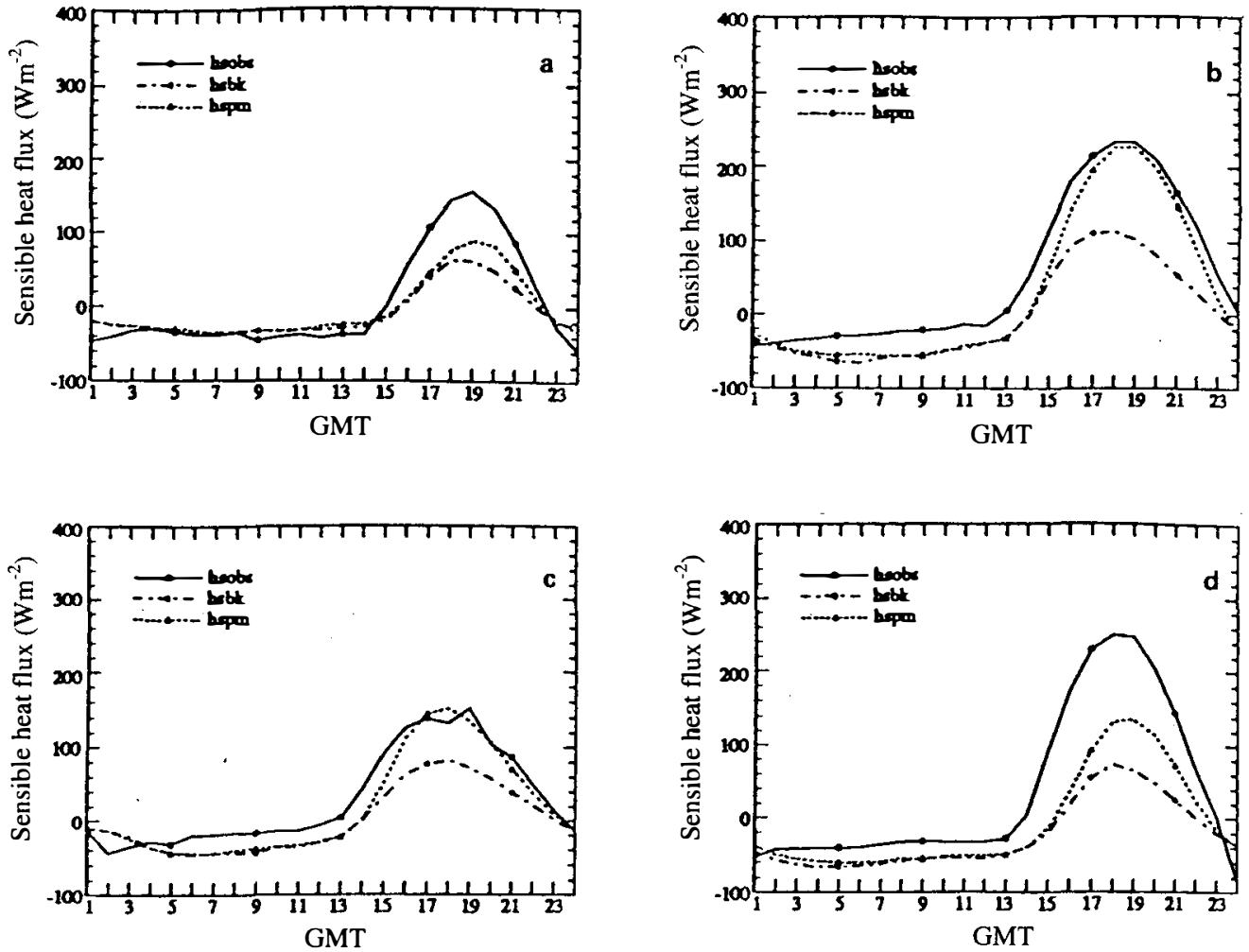


Fig. 4.1. Hourly average of model estimation of sensible heat flux (Wm^{-2}) in (a) January; (b) April; (c) July; and (d) October, 1995 during the model's 1-24 hr forecast period. The solid lines stand for the corresponding observation from the SGP ARM site, dashed lines for the model with the bucket method and the dotted lines for the model with the PM method.

respectively.

Due to the inappropriate simulation of skin temperature, SHF is not well simulated by the model with the bucket method (Figure 4.1). This method tends to underestimate SHF during the daytime and conversely to overestimate it during the nighttime. In other words, the model's ground surface temperature is too warm during the nighttime and too cold during the daytime. The mean daytime SHF are 10 and 21 Wm^{-2} for the model using the bucket and PM methods, respectively, in January. The corresponding observations show a mean SHF of 45 Wm^{-2} in January. In addition, the daytime variation of SHF is better captured (doubled and closer to the observation) by the model when the PM method is in use in April and July. Neither the bucket nor the PM methods make an accurate prediction of SHF for the nighttime and daytime in October although the PM method helps the model make some minor improvements in the simulation of daytime SHF. The mean daytime SHF are 10 and 38 Wm^{-2} for the model with the bucket and PM methods, respectively, in October. The corresponding observations show a

Table 4.1. Percentage and RMS errors of model estimations of sensible heat flux in (a) January; (b) April; (c) July; and (d) October 1995 during the model's 1-24 hr forecast period. Night is defined as from 01Z to 12Z, day from 13Z to 24Z and the total from 01Z to 24Z.

	Bucket method			PM method		
	night	day	total	night	day	total
(a) January						
% error	-21.2	-76.9	-404.0	-23.2	-53.6	-232.0
RMS error	10.9	54.0	38.9	11.6	40.9	30.1
(b) April						
% error	91.4	-63.1	-102.4	76.7	-21.1	-46.0
RMS error	28.3	90.8	67.2	25.5	31.6	28.7
(c) July						
% error	56.7	-55.8	-98.4	51.9	-15.5	-41.0
RMS error	21.9	48.3	37.5	20.2	20.9	20.6
(d) October						
% error	53.7	-90.5	-167.5	41.8	-65.3	-122.5
RMS error	22.2	122.2	87.9	18.9	89.2	64.5

mean SHF of 108 Wm^{-2} . The main reason for this difference is that it is predicted that the temperature gradient between the model's ground surface and lowest model level is much smaller than the corresponding observation, such that not enough heat can be emitted from the model's ground surface into the air in October. The mean daytime temperature gradients are -0.3 and $+0.2^\circ\text{C}$ for the model with the bucket and PM methods, respectively. The corresponding observations show a mean value of $+4.4^\circ\text{C}$. The model's lowest model level is warmer when SHF is greater owing to the use of the PM method (Figure 4.2). In April, the PM method results in a mean daytime temperature at the lowest model level of 16.5°C . The bucket method is associated with a mean daytime temperature at the lowest model level of 14.9°C . The corresponding observations reveal a mean value of 14.8°C in April.

The PM method tends to generate less LHF than the bucket method which means there is less moisture supply from the ground surface. This naturally leads to a reduced chance of low-level cloud formation. In this forecast period, there is a 26% possibility of low-level cloud formation in the model using the bucket method in January, but only a 16% possibility for low-level cloud formation in the model using the PM method during the same time period. This increases the possibility for incoming shortwave and longwave radiation to reach the model's ground surface during the daytime. Net radiation at the ground surface (R_{net}) during

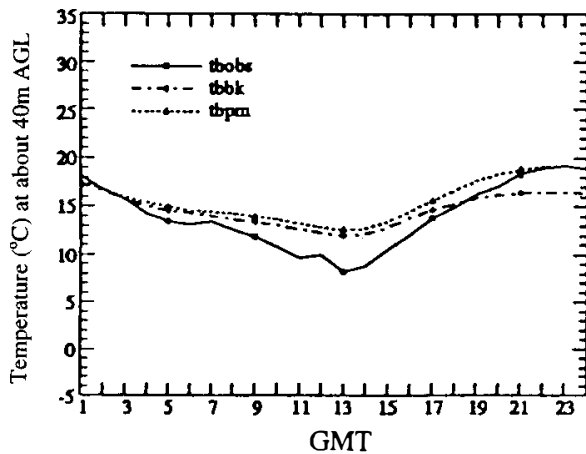


Fig. 4.2. Same as Figure 4.1 but for the model estimation of temperature ($^{\circ}\text{C}$) at the lowest model level (about 40m AGL) in April 1995.

Table 4.2. Same as Table 4.1 but for the model estimation of temperature ($^{\circ}\text{C}$) at the lowest model level (about 40m AGL) in April 1995.

	Bucket method			PM method		
	night	day	total	night	day	total
% error	7.9	0.9	4.2	11.0	11.6	11.3
RMS error	1.5	2.2	1.9	1.9	2.2	2.1

the daytime is then expected to be greater when the PM method is utilized. As shown in Figure 4.4 and Table 4.4, mean daytime R_{net} is adjusted from an underestimation of 3% (bucket method) to an overestimation of 4% (PM method) in January. R_{net} is increased by 20% via the use of the PM method in April. Both the PM and bucket methods contribute to an outstanding prediction of R_{net} in October. With either method, the daytime forecast error of R_{net} in the model is less than 6% in October.

Less moisture is available at the ground surface when the PM method is in use which means that there is less moisture content in the model's lower atmosphere. The bucket method offers a better estimation of the mixing ratio at the lowest model level during the nighttime, while the PM method gives a more accurate estimation of the mixing ratio at the model's lowest level during the daytime in January (Figure 4.5a). The daily -nighttime plus daytime-average mixing ratio at the model's lowest level are 4.1 and 7.5 g/kg for the model with the bucket method in January and April, respectively, but the same ratios are 3.8 and 6.5 g/kg for the model with the PM method. The corresponding observations show mean values of 3.9 and 6.7 g/kg in January and April, respectively. The rapid increase in the mixing ratio at the lowest model level shown by the bucket method during the daytime of April is obviously dampened by the use of the PM method (Figure 4.5b). The model using the bucket method is skillful at predicting nighttime moisture content at 40m AGL, yet unable to predict the same trend for daytime in July (18.1 g/kg) (Figure 4.5c). In contrast, the PM method is associated with a much better simulation of the mixing ratio at 40m AGL during the daytime in July (15.7 g/kg). The corresponding observations show a mean value of 15.0 g/kg in July. Again, the model's

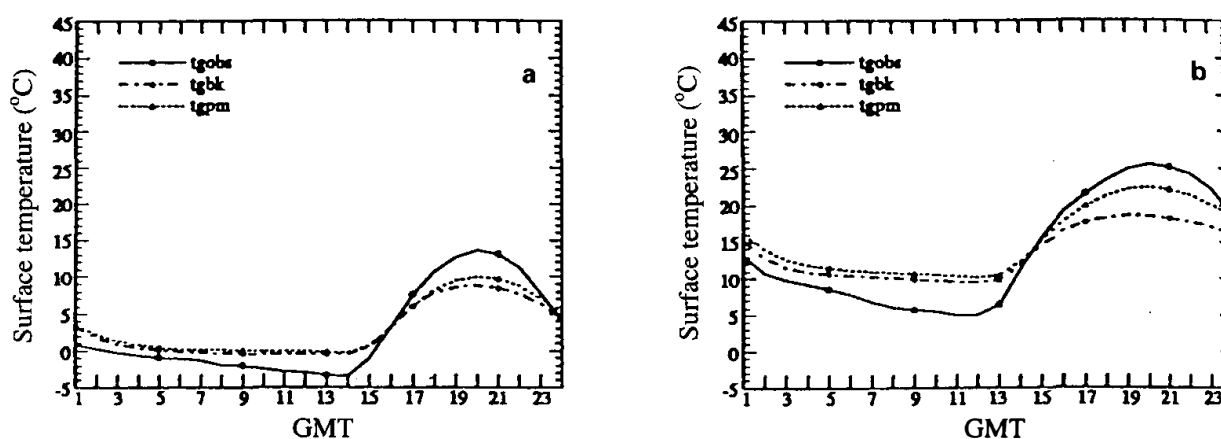


Fig. 4.3. Same as Figure 4.1 but for the model estimations of ground surface (skin) temperature ($^{\circ}\text{C}$) in (a) January and (b) April 1995.

Table 4.3. Same as Table 4.1 but for model estimations of ground surface (skin) temperature ($^{\circ}\text{C}$) in (a) January and (b) April 1995.

	Bucket method			PM method		
	night	day	total	night	day	total
(a) January						
% error	127.9	-20.0	6.9	159.1	-10.9	26.0
RMS error	1.7	3.0	2.5	2.1	2.5	2.3
(b) April						
% error	40.0	-18.3	-1.9	50.9	-6.2	9.9
RMS error	3.3	4.8	4.1	4.1	2.4	3.3

forecast of mixing ratio at 40m AGL in October (Figure 4.5d) is evidently improved by the use of PM method (7.2 g/kg). The bucket method leads to a moistening of the lowest model level atmosphere, which is very unrealistic (8.0 g/kg). The corresponding observations show a mean value of 6.5 g/kg in October.

4.2 For 25-48 hr and 49-72 hr Forecast Periods

During the 25-48 hr forecast period, the bucket method has a tendency to overestimate LHF by 70%, 11%, 6% and 63% during the daytime in January, April, July and October, respectively (Figure 3.4 and Table 3.2). The PM method, on the other hand, causes the model to overestimate LHF by only 63%, 3% and 37%, in January, April and October, respectively, and underestimate LHF by 14% in July. The main reason for this underestimation is that the

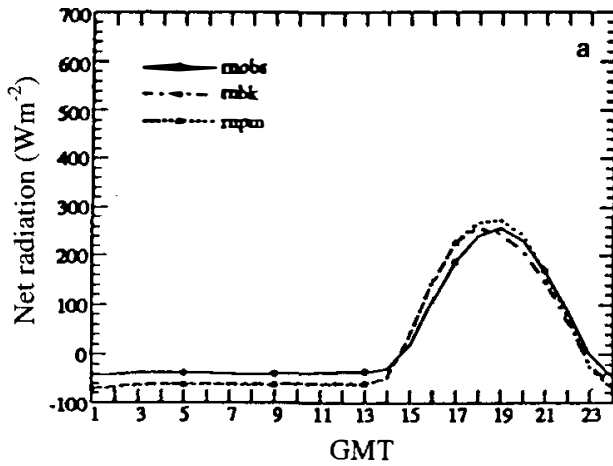


Fig. 4.4. Same as Figure 4.1 but for model estimations of net radiation at the ground surface (Wm^{-2}) in (a) January; (b) April; and (c) October 1995.

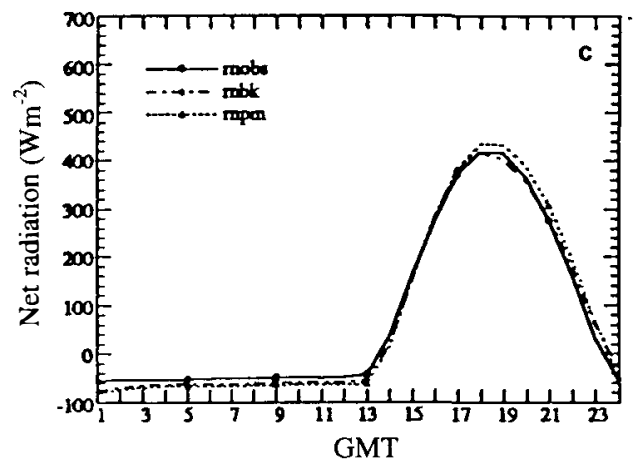
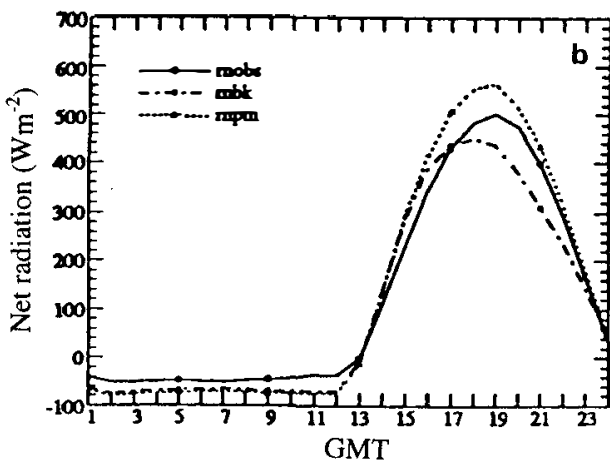


Table 4.4. Same as Table 4.1 but for model estimations of net radiation at the ground surface (Wm^{-2}) in (a) January, (b) April and (c) October 1995.

	Bucket method			PM method		
	night	day.	total	night	day	total
(a) January						
% error	56.8	- 3.2	-41.6	62.1	4.1	-33.1
RMS error	22.2	24.6	23.4	24.2	25.1	24.7
(b) April						
% error	49.1	- 6.4	-16.8	61.5	14.0	5.1
RMS error	23.1	51.2	39.7	28.5	48.8	40.0
(c) October						
% error	22.5	1.2	-6.0	32.7	5.6	-3.5
RMS error	11.9	15.7	13.9	16.9	22.4	19.8

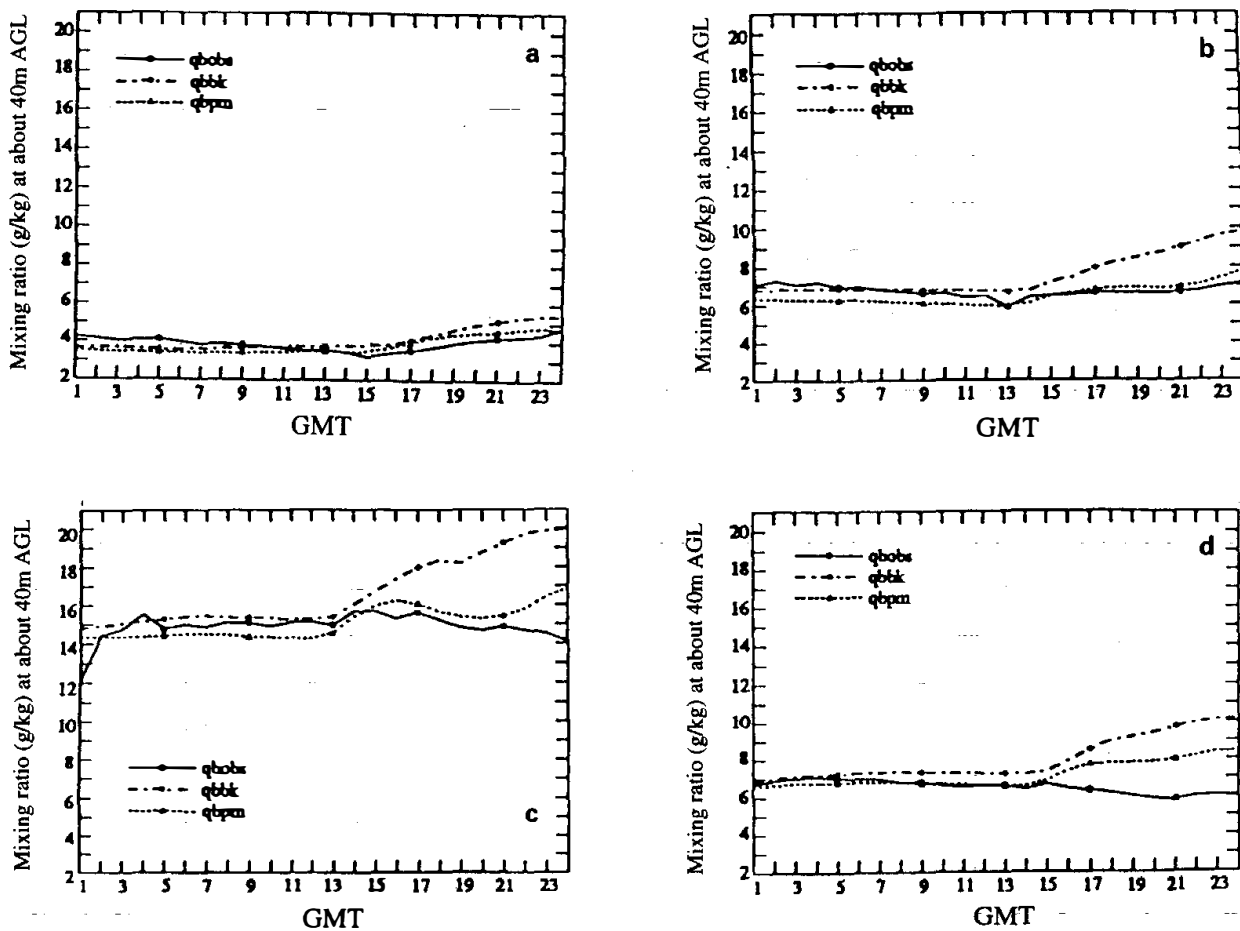


Fig. 4.5. Same as Figure 4.1 but for model estimation of mixing ratio (g/kg) at the lowest model level in (a) January; (b) April; (c) July and (d) October 1995.

stomatal resistance (90 s m^{-1}) used in this study is too large for the growing season. The mean daytime R_{net} are 334 and 349 W m^{-2} for the model with the bucket and PM method, respectively. The corresponding observations show a mean value of 379 W m^{-2} . It should be stated that the daytime mean PE (358 W m^{-2}) estimated by the bucket method exceeds the mean daytime R_{net} in the model during the same period. This is a very unrealistic feature and is one of the major flaws of the bucket method. Neither the bucket nor the PM method can make a good estimation of daytime SHF in January. Both methods lead to an underestimation of daytime SHF although the PM method does show some improvement (Figure 4.7). The mean daytime SHF are estimated to be 8 and 13 W m^{-2} using the bucket and PM methods, respectively, in January. The corresponding observations reveal a mean SHF of 44 W m^{-2} . It is suggested that the main reason for this error is that the temperature gradient between the ground surface and lowest model level is in the opposite direction from the corresponding observation. The model with both the bucket and PM methods shows a mean daytime temperature gradient of -1.0°C in January. The observations reveal a mean temperature gradient of $+2.5^\circ\text{C}$. When compared to the bucket method, the mean daytime SHF, in April, generated by the model is doubled (from 57 to 119 W m^{-2}) and is very similar to the corresponding observation

Table 4.5. Same as Table 4.1 but for model estimations of the mixing ratio (g/kg) at the lowest model level in (a) January; (b) April; (c) July; and (d) October 1995.

	Bucket method			PM method		
	night	day	total	night	day	total
(a) January						
% error	-6.7	16.7	5.0	-12.1	7.1	-2.5
RMS error	0.3	0.7	0.6	0.5	0.3	0.4
(b) April						
% error	-0.7	25.5	12.1	-9.8	3.2	-3.4
RMS error	0.3	1.9	1.3	0.7	0.3	0.5
(c) July						
% error	3.3	20.8	12.1	-2.4	4.9	1.3
RMS error	0.9	3.6	2.6	0.9	1.1	1.0
(d) October						
% error	5.5	41.6	22.7	-2.1	22.6	9.7
RMS error	0.4	2.9	2.1	0.2	1.6	1.2

(134 Wm⁻²) when the PM method is in effect. In October, the bucket method leads to a 47% overestimation of moisture content at the lowest model level (Figure 4.6). The PM method, in contrast, results in an overestimation of 17%, a significant degree of drying.

During the 49-72 hr forecast period, the bucket method has a tendency to overestimate LHF by 65%, 15% and 44% during the daytime in January, April and October, respectively, and to underestimate LHF by 10% in July (Figure 3.5 and Table 3.3). The PM method causes the model to overestimate LHF by only 51% and 27%, in January and October, respectively, but underestimate LHF by 10% and 11% in April and July, respectively. For the bucket method used for July, it is found that the skin temperature and the associated saturation surface mixing ratio are too low (Figure 4.8), while the lower atmosphere is too moist (the mixing ratio at the lower atmosphere is too high, see Figure 4.9) during this forecast period, such that the corresponding moisture gradient between the ground surface and lowest model level is 10-13 g/kg (or 50-60%) less than that from observation. This leads to a significant underestimation of the

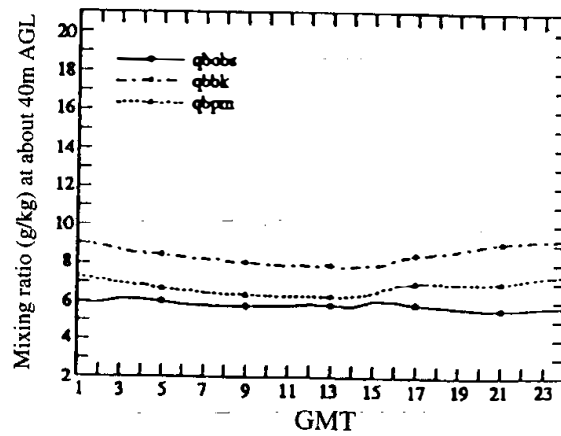


Fig. 4.6. Hourly average of model estimation of mixing ratio (g/kg) at the lowest model level in October 1995 during the model's 25-48 hr forecast period. The solid lines stand for the corresponding observation from the SGP ARM site, dashed lines for the model with the bucket method and the dotted lines for the model with the PM method.

Table 4.6. Percentage and RMS errors of the model estimation of the mixing ratio (g/kg) at the lowest model level in October 1995 during the model's 25-48 hr forecast period. Night is defined as from 01Z to 12Z, day from 13Z to 24Z and the total from 01Z to 24Z.

	Bucket method			PM method		
	night	day	total	night	day	total
% error	41.7	48.6	45.1	13.0	19.2	16.1
RMS error	2.5	2.9	2.7	0.8	1.2	1.0

potential ET by the bucket method, causing the ET to be reduced significantly in the model. In April and July, the PM method results in an underestimation of ET. The main reason is still that the stomatal resistance (90 s m^{-1}) used in this study is too large for the growing season.

5. SUMMARY AND CONCLUSIONS

The bucket method demonstrates the expected overestimation of LHF emitted from the model's ground surface. The PM method to estimate the potential ET over land area is introduced into the MM4 to solve this problem. Since the PM method sets an upper bound for the estimation of potential ET, the LHF estimated by the model is no longer too unreasonable. From the above discussion, six important facts are noted.

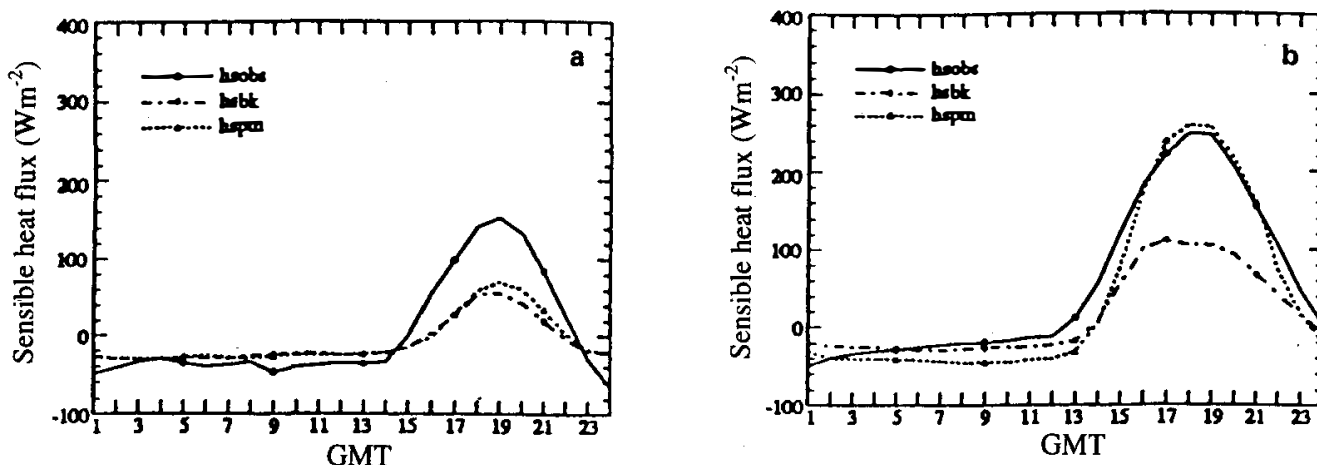


Fig. 4.7. Same as Figure 4.6 but for model estimations of sensible heat flux (Wm^{-2}) in (a) January and (b) April 1995.

Table 4.7. Same as Table 4.6 but for model estimations of sensible heat flux (Wm^{-2}) in (a) January and (b) April 1995.

	Bucket method			PM method		
	night	day	total	night	day	total
(a) January						
% error	-28.4	-81.7	-460.0	-29.3	-70.3	-362.1
RMS error	12.9	57.7	41.8	12.8	51.8	37.7
(b) April						
% error	-1.4	-57.7	-71.6	56.4	-10.9	-27.6
RMS error	11.9	87.7	62.6	20.4	28.0	24.5

- (1) For the first 24-hr forecast period, the model tends to severely overestimate LHF, especially in the cold season (January and October) due to the spinup effect resulting from the improper assignment of the initial skin temperature. Both the percentage and RMS errors to estimate LHF by the model decrease with increased forecasting time in accordance with the constraint of surface energy balance.
- (2) There is always ET coming from the model's surface during the nighttime while observations show near-zero ET in the same time period. This is due to an inappropriate simulation of the skin temperature as a result of the improper prediction of the lower atmospheric temperature.
- (3) The bucket method tends to make an estimation of PE that is not within the bounds of

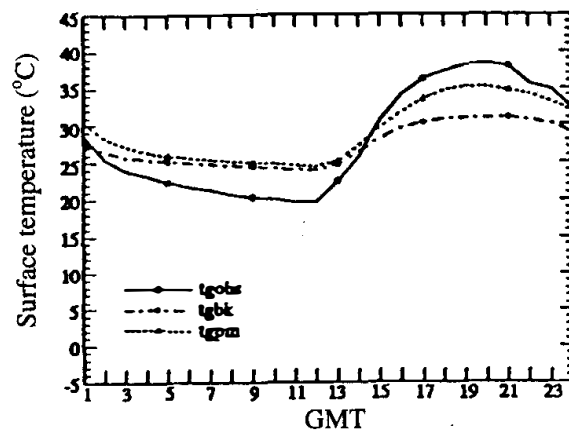


Fig. 4.8. Hourly average of model estimation of ground surface (skin) temperature ($^{\circ}\text{C}$) in July of 1995 during the model's 49-72 hr forecast period. The solid lines stand for the corresponding observation from the SGP ARM site, dashed lines for the model with the bucket method and the dotted lines for the model with the PM method.

Table 4.8. Percentage and RMS errors of model estimation of ground surface (skin) temperature ($^{\circ}\text{C}$) in July 1995 during the model's 49-72 hr forecast period. Night is defined as from 01Z to 12Z, day from 13Z to 24Z and the total from 01Z to 24Z.

	Bucket method			PM method		
	night	day	total	night	day	total
% error	12.8	-12.7	-2.5	17.2	-4.3	4.3
RMS error	3.2	5.2	4.3	3.9	2.3	3.2

energy balance at ground surface during the daytime in July. This is one of the major drawbacks of the bucket method.

- (4) The PM method can effectively reduce the degree of the model's overestimation of LHF for the months of January, April, July and October. The improvement is most significant during the first 24-hr forecast period. The assignment of stomatal resistance, given a fixed moisture availability, is crucial to whether the PM method overestimates or underestimates daytime LHF in different seasons. It is proposed that in a future study by the authors a canopy-soil model will be implemented into the numerical model to simulate the diurnal and seasonal variability of stomatal resistance to account for different soil types (and their relative wetness), vegetation types (leaf area index, etc.), etc. This will enable the stomatal resistance used in the model to realistically represent canopy transpiration, evaporation from wet canopy (dew, or precipitation intercepted by canopy), evaporation from ground soil and so on.

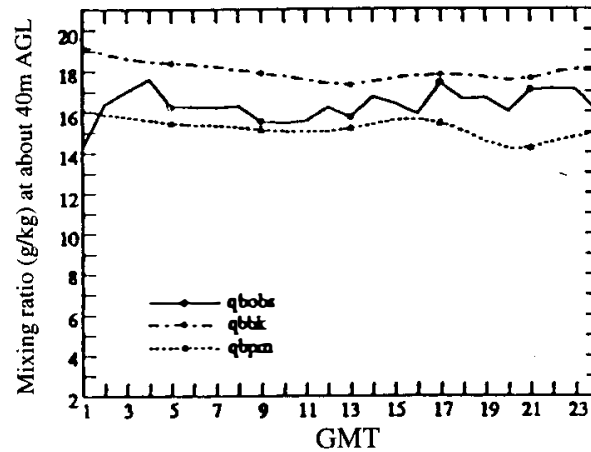


Fig. 4.9. Same as Figure 4.8 but for mixing ratio (g/kg) at the lowest model level in July 1995.

Table 4.9. Same as Table 4.8 but for mixing ratio (g/kg) at the lowest model level in July 1995.

	Bucket method			PM method		
	night	day	total	night	day	total
% error	13.4	7.1	10.2	-4.2	-9.6	-7.0
RMS error	2.4	1.3	1.9	1.1	1.8	1.5

- (5) Less surface evaporative cooling as implied by the PM method leads to a better estimation of skin temperature and SHF by the model, especially during the daytime. The PM method is associated with a higher temperature at the lowest model level due to more available SHF.
- (6) The model using the PM method better estimates the net radiation at ground surface due to a reduced chance of low-level cloud formation from a more reasonable moisture supply from the ground surface by the use of the PM method.

Acknowledgments The authors would like to thank Dr. Kelvin Droegemiere, director of the Center for Analysis and Prediction of Storms of the University of Oklahoma for his generous permission to allow the authors to use the IBM workstations to perform model simulations. This study was supported by the Atmospheric Radiation Measurement program.

REFERENCES

- Anthes, R. A., 1977: A cumulus parameterization scheme utilizing a one-dimensional cloud model. *Mon. Wea. Rev.*, **105**, 270-286.
- Anthes, R. A., and T. T. Warner, 1978: Development of hydrodynamic models suitable for air

- pollution and other mesometeorological studies. *Mon. Wea. Rev.*, **106**, 1045-1078.
- _____, E. Y. Hsie, and Y.-H. Kou, 1987: Description of the Penn State/NCAR mesoscale model version 4 (MM4). NCAR Tech. Note NCAR/TN-282+STR, 66pp.
- Beljaars, A. C. M., P. Viterbo, M. J. Miller, and A. K. Betts, 1996: The anomalous rainfall over the United States during July 1993: Sensitivity to land surface parameterization and soil moisture anomalies. *Mon. Wea. Rev.*, **124**, 362-383.
- Benoit, R., 1977: On the integral of the surface layer profile-gradient functions. *J. Appl. Meteor.*, **16**, 859-860.
- Betts, A. K., J. H. Ball, and A. C. M. Beljaars, 1993: Comparison between the land surface response of the ECMWF model and the FIFE-1987 data. *Quart. J. R. Meteor. Soc.*, **119**, 975-1001.
- Blackadar, A. K., 1976: Modeling the nocturnal boundary layer. Preprints of the third symposium on atmospheric turbulence, diffusion and air quality, Raleigh, NC, 19-22 October 1976, Amer. Meteor. Soc., Boston, 443-447.
- Bolton, D., 1980: The computation of equivalent potential temperature. *Mon. Wea. Rev.*, **108**, 1046-1053.
- Chen, C.-R., 1996: Improved treatment of surface evapotranspiration in a mesoscale numerical model. Ph. D. dissertation, University of Oklahoma, 236pp.
- Carlson, T. N., and F. E. Boland, 1978: Analysis of urban-rural canopy using a surface heat flux/temperature model. *J. Appl. Meteor.*, **17**, 998-1013.
- Deardorff, J. W., 1972: Parameterization of the planetary boundary layer for use in general circulation models. *Mon. Wea. Rev.*, **100**, 93-106.
- Dudhia, J., 1989: Numerical study of convection observed during the winter monsoon experiment using a mesoscale two-dimensional model. *J. Atmos. Sci.*, **46**, 3077-3107.
- Gillies, R. R., and T. Carlson, 1995: Thermal remote sensing of surface soil water content with partial vegetation cover for incorporation into climate models. *J. Appl. Meteor.*, **34**, 745-756.
- Manabe, S., 1969: Climate and the ocean circulation: I. The atmospheric circulation and the hydrology of the earth's surface. *Mon. Wea. Rev.*, **97**, 739-774.
- Mahrt, L., and M. Ek, 1984: The influence of atmospheric stability on potential evaporation. *J. Climate Appl. Meteor.*, **23**, 222-234.
- Milly, P. C. D., and K. A. Dunne, 1994: Sensitivity of the global water cycle to the water-holding capacity of land. *J. Climate*, **7**, 506-526.
- Monteith, J. L., 1965: Evaporation and environment. *Symp. Soc. Exp. Biol.*, **19**, 205-235.
- _____, 1975: Vegetation and the atmosphere. Vol. I, Principles. Academic Press, 278pp.
- Nappo, C. J., 1975: Parameterization of surface moisture and evaporation rate in a planetary boundary layer model. *J. Appl. Meteor.*, **14**, 289-296.
- Nickerson, E. C., and V. E. Smiley, 1975: Surface layer and energy budget parameterizations for mesoscale models. *J. Appl. Meteor.*, **14**, 297-300.
- Pan, H.-L., 1990: A simple parameterization scheme of evapotranspiration over land for the NMC medium-range forecast model. *Mon. Wea. Rev.*, **118**, 2500-2512.
- Pan, Z., E. Takle, M. Segal, and R. Turner, 1996: Influences of model parameterization schemes

- on the response of rainfall to soil moisture in the central United States. *Mon. Wea. Rev.*, **124**, 1786-1802.
- Paulson, C. A., 1970: The mathematical representation of wind speed and temperature in the unstable atmospheric surface layer. *J. Appl. Meteor.*, **9**, 857-861.
- Penman, H. L., 1948: Natural evaporation from open water, bare soil, and grass. *Proc. Roy. Soc. Ser. A.*, **193**, 120-195.
- Segal, M., R. W. Arritt, C. Clark, R. Rabin, and J. M. Brown, 1995: Scaling evaluation of the effect of surface characteristics on potential for deep convection over uniform terrain. *Mon. Wea. Rev.*, **123**, 383-400.
- Shukla, J., and Y. Mintz, 1982: Influence of land-surface evapotranspiration on the earth's climate. *Science*, **215**, 1498-1501.
- Stokes, G. M., and S. E. Schwartz, 1994: The atmospheric radiation measurement (ARM) program: Programmatic background and design of the cloud and radiation test bed. *Bull. Amer. Meteor. Soc.*, **75**, 1201-1221.
- Taconet, O., T. Carlson, R. Bernard and D. Vidal-Madjar, 1986: Evaluation of a surface/vegetation parameterization using satellite measurements of surface temperature. *J. Appl. Meteor.*, **25**, 1752-1767.
- Tanner, C. B., and W. G. Pelton, 1960: Potential evapotranspiration estimated by the approximate energy balance method of Penman. *J. Geophys. Res.*, **65**, 3391-3412.
- Walker, J., and P. R. Rowntree, 1977: The effect of soil moisture on circulation and rainfall in a tropical model. *Quart. J. Roy. Meteor. Soc.*, **103**, 29-46.
- Wetzel, P. J., and J.-T. Chang, 1988: Evapotranspiration from nonuniform surfaces: A first approach for short-term numerical weather prediction. *Mon. Wea. Rev.*, **116**, 600-621.
- Yeh, T.-C., R. T. Wetherald, and S. Manabe, 1984: The effect of soil moisture on the short-term climate and hydrology change - A numerical experiment. *Mon. Wea. Rev.*, **112**, 474-490.